Growth Dynamics of Self-Assembled Monolayers in Dip-Pen Nanolithography

Yoonho Ahn,[†] Seunghun Hong,[‡] and Joonkyung Jang*,[†]

School of Nano Science & Technology, Pusan National University, Busan, Republic of Korea 609-735, and Physics and Nano-Systems Institute, Seoul National University, Seoul, Republic of Korea 151-747

Received: October 11, 2005; In Final Form: January 9, 2006

Using molecular dynamics simulations, we studied the growth mechanism of self-assembled monolayers in dip-pen nanolithography. A molecule dropping from the tip kicks out a molecule sitting on the substrate, and the displaced molecule in turn kicks out a molecule next to it. This kicking propagates and finally stops when it hits the periphery of the monolayer. This monolayer growth is faster than predicted from the previous diffusion theory. Increasing the molecule−substrate binding strength enhances the molecular deposition rate and makes the monolayer well-ordered.

1. Introduction

Dip-pen nanolithography (DPN)[1] has proven to be a useful tool for creating nanoscale patterns on various substrates. In DPN, an atomic force microscope (AFM) tip serves as a source of molecular "ink" that eventually forms a self-assembled monolayer (SAM) on a substrate. Despite its widespread applications,[1−5] little is known about the molecular mechanism of the SAM growth in DPN. This fundamental aspect is important in understanding exactly how DPN is influenced by the tip scan speed, temperature, and humidity.[6−8] There have been several theoretical models proposed to explain the dynamics of DPN.[8,9] These phenomenological theories however lack a molecular foundation and cannot reveal the real-time dynamics of DPN. Herein, we use molecular dynamics (MD) simulation to reveal the mechanism and dynamics of a monolayer growth in DPN. Significantly, we systematically vary the molecule−substrate binding strength to examine how it affects the monolayer formation.

2. Simulation Details

We considered the monolayer growth on an Au(111)-like surface. Ink molecules are taken to be nonpolar and spherical. The masses of the ink molecules are set to that of 1-octadecanethiol, $CH_3(CH_2)_{17}SH$ (ODT), a prototypical molecule in DPN. We placed 286 ink molecules inside an inverted cone made of fictitious atoms with an approximate size of silicon. The cone has a radius and a height of 3.3 and 4.8 nm, respectively. We equilibrated the molecules inside the cone by running a 300-ps-long MD trajectory (see below). We then eliminated the bottom part of the inverted cone to obtain an inverted truncated cone with a bottom radius of 1.5 nm. The truncated cone consists of 297 silicon-like atoms. Ink molecules can pass through the bottom hole and further move down to the substrate. This tip pertains to the so-called "fountain pen" recently used in DPN.[10] The substrate mimics gold (face-centered cubic (fcc), lattice parameter of 2.88 Å), and its surface is taken to be (111). Only the top two layers of the gold lattice are included in the simulation. The lateral size of the substrate is 15 nm by 15 nm (6353 Au atoms in total). We fixed the tip in position, and the vertical distance from the tip end to the substrate surface was 1.3 nm.

The interatomic and intermolecular (ink−ink) interactions are of the Lennard-Jones (LJ) type, $U(r) = 4\epsilon[(\sigma/r)^{12} - (\sigma/r)^6]$, where ϵ is the potential well depth, σ is the collision diameter, and r is the distance between two atoms or molecules.[11] We set ϵ of the ink molecule equal to that of stearic acid ethyl ester ($C_{20}H_{40}O_2$), which is similar to ODT in mass.[12] We chose $\sigma =$ 4.99 Å for the ink molecule to reproduce the well-known structure of the ODT monolayer on Au(111).[13] The tip atom has a σ value close to that of silicon ($\sigma = 4.0$ Å), but its ϵ (0.1 kcal/mol) is set to be 4 times smaller than that of Si[14] to achieve an easy flow of ink molecules from the tip. The LJ parameters for gold ($\epsilon = 1.0$ kcal/mol, $\sigma = 2.655$ Å) are taken from the literature.[15] The Lorentz−Berthelot combination rule[11] was used for the interactions between unlike atomic or molecular species. We characterize the binding strength between the molecule and the substrate in terms of the potential well depth for the molecule−substrate LJ potential. We call the well depth the *molecule−substrate binding strength* ϵ_b (1.1 kcal/mol). We considered various energetic parameters for the substrate. We ran simulations using a range of ϵ_b values (1.1, 2.2, 4.4, 6.3, 8.8, and 12.6 kcal/mol) to check the effects of ϵ_b on the monolayer growth. We propagated the molecular trajectory by using the velocity Verlet algorithm.[11] We fixed the AFM tip and substrate atoms in simulation. We used a time step of 3 fs, and the total time length of simulation was 600 ps. The temperature of our system was fixed to 300 K by using the thermostat proposed by Berendsen et al.[16]

Our model of the ink molecule can be viewed as a highly coarse-grained version of ODT. To assess the validity of the model, we have performed a simulation that explicitly takes into account the alkyl chain of ODT as well as the sulfur−Au interaction. The Au−S interaction is described as a pairwise additive Morse potential.[17−19] We used the well depth of the Morse potential D_e (3.182 kcal/mol) fitted to the experimental binding energy of ODT (−44.0 kcal/mol).[20] Since D_e is similar to ϵ_b, we expect the Au−S binding strength of ODT lies somewhere between $\epsilon_b = 2.2$ and 4.4 kcal/mol in the present simulation. As shown in the following, the mechanism of the

* Author to whom correspondence should be addressed. E-mail: jkjang@pusan.ac.kr.
[†] Pusan National University.
[‡] Seoul National University.

10.1021/jp055778r CCC: $33.50
Published on Web 02/08/2006

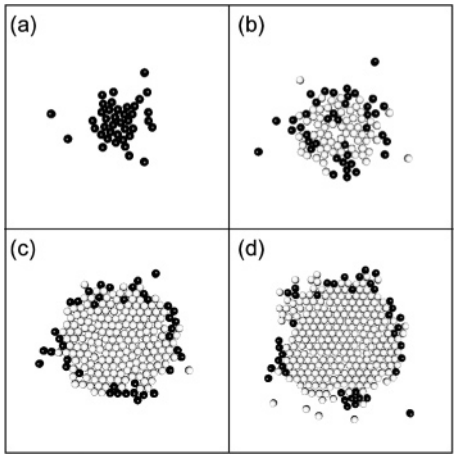

Figure 1. Snapshots of ink molecules deposited on the substrate. The molecule−substrate binding strength ϵ_b is 6.3 kcal/mol. For visual clarity, we do not show either tip and substrate atoms or the molecules on top of the monolayer. Each molecule in the figure is near one of the 3-fold hollow sites of the substrate surface, fcc (111). Snapshots are taken at $t = 12$ ps (a), 60 ps (b), 168 ps (c), and 600 ps (d). Molecules deposited at $t = 12$ ps and at later times are drawn as dark and bright spheres, respectively.

monolayer growth in such a realistic simulation agrees with the present simulation. It is also encouraging to note that Mahaffy et al. showed that coarse-graining butanethiolate as a spherical molecule yields a nearly identical value in its surface diffusion constant on the Au(111) surface.[18]

3. Results and Discussion

Figure 1 illustrates the molecular mechanism of the SAM growth. Shown are snapshots of a growing monolayer (ϵ_b = 6.3 kcal/mol) taken at time 12 ps (Figure 1a), 60 ps (Figure 1b), 168 ps (Figure 1c), and 600 ps (Figure 1d). Molecules deposited at time 12 ps (Figure 1a) are drawn as dark spheres, and the bright spheres represent molecules deposited at later times. For visual clarity, we removed the tip and substrate from the figure. (The tip is located at the center of each figure.) Also, the molecules above the monolayer are not shown. Each molecule is sitting near one of the 3-fold hollow sites of the substrate surface, fcc (111). The figures show that molecules initially deposited at the center move toward the periphery on the bare surface. In more detail, an incoming molecule from the tip kicks a molecule on the substrate out of its place, and the molecule just kicked out in turn pushes molecules next to it, and so on. This kicking propagates until it hits the periphery of the monolayer and finally stops. The kicking stops because the molecule at the periphery has no molecule to push away from the center. As long as there are incoming molecules from the tip, the kicking continues. (Depending on ϵ_b, this time varies from ~250 to 600 ps.) This dynamics is in stark contrast to the assumption made in the previous diffusion model.[9] It assumes that molecules dropping from the tip are trapped as soon as they hit the bare surface (due to the strong molecular binding to the substrate). And molecules diffuse only on the monolayer already formed by the molecules deposited at earlier times. At longer times than considered here, the above "kicking" needs to propagate farther to reach the periphery (due to a larger size of the monolayer). Molecules then might opt to move on top of the monolayer, instead of kicking many molecules in the monolayer. This point however needs further investigation. The above kicking mechanism is also observed in the simulation that explicitly takes into account the chain structure of ODT

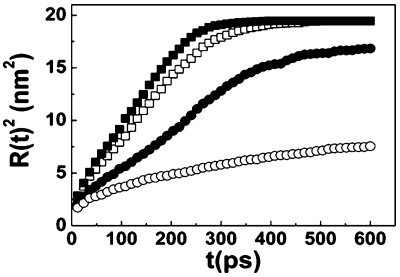

Figure 2. Radial growth of the monolayer for various molecule−substrate binding strengths, ϵ_bs. The radius squared of a monolayer, $R(t)^2$, is plotted as a function of time for $\epsilon_b = 1.1$ (open circles), 2.2 (filled circles), 4.4 (open squares), and 6.3 (filled squares) kcal/mol.

(Supporting Information). Our observation agrees with the previous report that alkanethiols move easily between adjacent hollow sites of Au (111) at a submonolayer coverage.[17] This has been ascribed to the fact that the barrier to movement of the thiol between hollow sites is small.

We quantitatively examine the dynamics of the monolayer growth. Suppose the number of molecules that form a monolayer at time t is $N(t)$. Then the *monolayer radius* can be defined as $R(t)^2 = N(t)/(\pi\rho)$, where ρ is the surface density of the monolayer (4.64 nm^{-2}). To count $N(t)$, we sorted out molecules whose vertical distances from the substrate surface are within 0.45 nm. Among such molecules, we checked the intermolecular distance of every possible pair and declared the pairs with intermolecular distances below 0.95 nm as neighbors. A molecule is treated as a part of the monolayer if it is a neighbor of *any* molecule that forms the monolayer.

In Figure 2, we plot the monolayer radius squared, $R(t)^2$, for various binding strengths. (Each radius was obtained by averaging over five independent runs.) Overall, $R(t)^2$ grows with time, and increasing the binding strength gives a faster growth in the radius. For $\epsilon_b = 1.1$ kcal/mol (open circles), $R(t)^2$ increases roughly linearly with time. The growth rate for $\epsilon_b = 2.2$ kcal/mol (filled circles) is larger at times under 400 ps. At the highest two binding strengths, $\epsilon_b = 4.4$ (open squares) and 6.3 (filled squares) kcal/mol, we see an approximately linear growth of $R(t)^2$ at short times and then a slower radial growth at later times that eventually stops. The cease of growth is due to the fact that all the molecules are deposited from the tip (no more incoming molecular flux from the tip). We found that raising ϵ_b above 6.3 kcal/mol makes no difference in the radial growth.

The previous diffusion theory[9] supposes that molecules irreversibly bind to the substrate and they only move on top of a monolayer. By treating the tip as a molecular source with a constant deposition rate n, one can derive the exact solution for the monolayer radius as

$$R(t)^2 = \lambda^2 4Dt \tag{1}$$

where D is the molecular diffusion constant. Here, λ^2 is determined from the equation $e^{-\lambda^2} = 4D\lambda^2/(n/\pi\rho)$. We can calculate the input parameters for the theory, n and D, as follows. We checked the number of molecules that pass through the bottom hole of the tip. Then the number of such molecules is fitted to a linear function of time, and the slope of the fit is taken to be the deposition rate.

In Figure 3a, we plot the deposition rate n for various molecule−substrate binding strengths ϵ_bs. Increasing ϵ_b makes the deposition faster due to the enhanced attraction from the substrate. The deposition rate levels off at high values of ϵ_b. We now turn to the diffusion constant, D. Note D refers to a molecular motion *over* a monolayer and must be independent

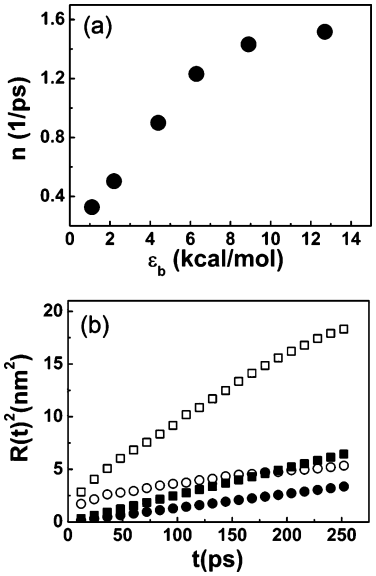

Figure 3. (a) Molecular deposition rate, n, vs the molecule−substrate binding strength, ϵ_b. (b) Comparison between MD simulation and the diffusion theory. The radius squared of a monolayer, $R(t)^2$, from simulation (open symbols) is compared to the prediction of the diffusion theory (filled symbols) for $\epsilon_b = 1.1$ (circles) and 6.3 (squares) kcal/mol.

of the molecular flux from the tip.[9] We thus ran a separate simulation without the tip just to calculate D. We spread an ink monolayer that completely covers the substrate and then place 20 ink molecules on top of the monolayer. We calculated D by using the Einstein relation,[11] $4Dt = \langle|\vec{\mathbf{r}}(t) - \vec{\mathbf{r}}(0)|^2\rangle$, where $\vec{\mathbf{r}}(t)$ is the lateral position of a molecule at time t. The diffusion constants obtained this way are 5.26×10^{-5} and 4.15×10^{-5} cm^2/s for $\epsilon_b = 1.1$ and 6.3 kcal/mol, respectively.

Using the above deposition rate and diffusion constant, we can calculate $R(t)^2$ from the diffusion theory, eq 1. In Figure 3b, the diffusion theory results (filled symbols) are compared to our MD simulation (open symbols) for $\epsilon_b = 1.1$ (circles) and 6.3 (squares) kcal/mol. The pattern growth in the MD simulation is faster than predicted by the diffusion theory. This discrepancy seems natural because the basic assumption of the diffusion theory (irreversible molecular binding to the substrate) breaks down in our simulation. Another shortcoming of the diffusion theory is that it inherently neglects the inertial effects of molecular motion. Diffusion assumes that molecules undergo many collisions before moving an appreciable distance, and molecules have no memory of their previous velocities. This Markovian assumption breaks down for an inertial limit where molecules move freely without any collision (like in a very dilute medium) and have complete memories of their previous velocities. The real molecular motion of course lies somewhere between the diffusion and inertial limits. If there is an improved theory that takes into account the inertial effects, then the radial growth from such theory will be faster than the diffusion theory and therefore will be closer to MD results.

Figure 4 shows the final ($t = 600$ ps) monolayer pattern for various molecule−substrate binding strengths, ϵ_bs. The tip and substrate atoms are omitted, and molecules are located near the 3-fold hollow sites of the fcc (111) surface. It is clear that the molecule−substrate binding strength greatly influences the final pattern. The monolayer pattern for $\epsilon_b = 1.1$ kcal/mol (Figure 4a) has some branches, reminding us of the experimental 1-dodecylamime monolayer on mica.[21] Increasing ϵ_b gives a roughly circular pattern as shown in Figures 4b ($\epsilon_b = 2.2$ kcal/mol) and 4c ($\epsilon_b = 4.4$ kcal/mol). There are however holes in

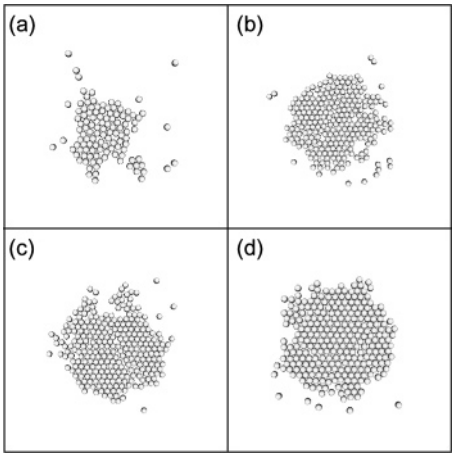

Figure 4. Final patterns of the ink monolayer. The monolayer pattern formed at $t = 600$ ps is shown for the molecule−substrate binding strengths ϵ_bs of 1.1 (a), 2.2 (b), 4.4 (c), and 6.3 (d) kcal/mol.

the SAM. With a further increase in ϵ_b, the monolayer eventually becomes compact and well-ordered (Figure 4d, $\epsilon_b = 6.3$ kcal/mol).

4. Concluding Remarks

In summary, our MD simulation reveals the molecular mechanism of the monolayer growth in DPN. Our results demonstrate that the previous diffusion theory fails to capture the essential features of the growth dynamics at the early stage (times less than 600 ps). Significantly, we have examined how the strength of molecular binding to the substrate affects the shape and dynamics of the monolayer growth. The monolayer grows faster and its pattern becomes more compact as the binding strength rises. Interestingly, the previous DPN experiment using a silazane molecule has reported a strong substrate dependence.[22]

In this work, we have focused on a nonpolar ink molecule with a spherical shape. Therefore, our model cannot address the effects of the internal structure of the ink molecule (for example, the orientation of the alkyl chain of an alkanethiol). We have shown, however, that as long as the molecule−substrate interaction energy is properly considered, this coarse-grained model captures the essential features of the growth dynamics in DPN.

Under nonvacuum conditions, a water meniscus[1,23] naturally forms between the tip and the substrate. Our results show that, in the absence of a meniscus, molecules can form a monolayer due to the attractive force from the substrate. This is in accord with the DPN experiments reporting SAM formation in a vacuum.[7,8] Under humid conditions however, the water meniscus will play an important role in DPN. Ink molecules will experience a strong capillary force[24] due to the meniscus. The meniscus can assist or impede the molecular transport depending on whether the molecule is hydrophilic or hydrophobic. It would be interesting to investigate how the meniscus affects DPN at the molecular level.

Acknowledgment. This work is supported by the Korean Research Foundation Grant No. KRF-2004-042-C00063.

Supporting Information Available: A movie illustrating the molecular dynamics simulation of the ODT monolayer growth on Au(111) (drawn as yellow spheres). Initially, 183 ODT molecules are attached to a silicon tip (drawn as magenta spheres). One can see that molecules located near the center of

the Au(111) surface are pushed away by incoming molecules toward the periphery of the substrate. The methyl groups and sulfur atoms of ODT are represented as blue and red spheres, respectively. The total time duration is 800 ps, and the simulation time step is 1 fs. The temperature is 300 K. We used a united atom model[14] for the methyl groups of ODT. According to ref 14, we fix the interatomic distances ($S-CH_2$, CH_2-CH_2, CH_3-CH_2) of ODT, but the torsional and bending motions are allowed. The LJ parameters for the atoms of ODT are taken from the work of Hautman and Klein.[25] The LJ parameters for the tip (Si) and gold atoms are taken from refs 14 and 15, respectively. The Au−S binding is modeled as the Morse potential reported by Zhang et al.[19] This material is available free of charge via the Internet at http://pubs.acs.org.

References and Notes

(1) Ginger, D. S.; Zhang, H.; Mirkin, C. A. *Angew. Chem., Int. Ed.* **2004**, *43*, 30.
(2) Wilson, D. L.; Martin, R.; Hong, S.; Cronin-Golomb, M.; Mirkin, C. A.; Kaplan, D. L. *Proc. Natl. Acad. Sci. U.S.A.* **2001**, *98*, 13660.
(3) Su, M.; Dravid, V. P. *Appl. Phys. Lett.* **2002**, *80*, 4434.
(4) Maynor, B. W.; Li, J.; Lu, C.; Liu, J. *J. Am. Chem. Soc.* **2004**, *126*, 6409.
(5) Bullen, D.; Chung, S.-W.; Wang, X.; Zou, J.; Mirkin, C. A.; Liu, C. *Appl. Phys. Lett.* **2004**, *84*, 789.
(6) Weeks, B. L.; Noy, A.; Miller, A. E.; DeYoreo, J. J. *Phys. Rev. Lett.* **2002**, *88*, 255505.
(7) Rozhok, S.; Piner, R. D.; Mirkin, C. A. *J. Phys. Chem. B* **2003**, *107*, 751.
(8) Sheehan, P. E.; Whitman, L. J. *Phys. Rev. Lett.* **2002**, *88*, 156104.
(9) Jang, J.; Hong, S.; Schatz, G. C.; Ratner, M. A. *J. Chem. Phys.* **2001**, *115*, 2721.
(10) Deladi, S.; Tas, N. R.; Berenschot, J. W.; Krijnen, G. J. M.; de Boer, M. J.; de Boer, J. H.; Peter, M.; Elwenspoek, M. C. *Appl. Phys. Lett.* **2004**, *85*, 5361.
(11) Allen, M. P.; Tildeseley, D. J. *Computer Simulation of Liquids*; Oxford University Press: New York, 1987.
(12) Zhou, J.; Lu, X.; Wang, Y.; Shi, J. *Fluid Phase Equilib.* **2000**, *172*, 279.
(13) Alves, C. A.; Smith, E. L.; Porter, M. D. *J. Am. Chem. Soc.* **1992**, *114*, 1222.
(14) Zhang, L.; Jiang, S. *J. Chem. Phys.* **2002**, *117*, 1804.
(15) Zhang, L.; Balasundaram, R.; Gehrke, S. H.; Jiang, S. *J. Chem. Phys.* **2001**, *114*, 6869.
(16) Berendsen, H. J. C.; Postma, J. P. M.; van Gunsteren, W. F.; DiNola, A.; Haak, J. R. *J. Chem. Phys.* **1984**, *81*, 3684.
(17) Beardmore, K. M.; Kress, J. D.; Gronbech-Jensen, N.; Bishop, A. R. *Chem. Phys. Lett.* **1998**, *286*, 40.
(18) Mahaffy, R.; Bhatia, R.; Garrison, B. J. *J. Phys. Chem. B* **1997**, *101*, 771.
(19) Zhang, L.; Goddard, W. A., III.; Jiang, S. *J. Chem. Phys.* **2002**, *117*, 7342.
(20) Dubois, L. H.; Nuzzo, R. G. *Annu. Rev. Phys. Chem.* **1992**, *43*, 437.
(21) Manandhar, P.; Jang, J.; Schatz, G. C.; Ratner, M. A.; Hong, S. *Phys. Rev. Lett.* **2003**, *90*, 115505.
(22) Ivanisevic, A.; Mirkin, C. A. *J. Am. Chem. Soc.* **2001**, *123*, 7887.
(23) Jang, J.; Schatz, G. C.; Ratner, M. A. *Phys. Rev. Lett.* **2004**, *92*, 085504.
(24) Jang, J.; Schatz, G. C.; Ratner, M. A. *J. Chem. Phys.* **2004**, *120*, 1157.
(25) Hautman, J.; Klein, M. L. *J. Chem. Phys.* **1989**, *91*, 4994.